RESEARCH REVIEW JOURNALS
Volume-04
Issue-02
February-2019

ISSN: 2455-3085 (Online)
RESEARCH REVIEW International Journal of Multidisciplinary
www.rrjournals.com[UGC Listed Journal]

A simple and fast method based on DWT and image texture for detection of splicing forgery in images

Mushtaq Saba

Assistant Professor Department Of Electronics and Communication Engineering, National Institute of Technology, Srinagar(India)

ARTICLE DETAILS

Article History
Published Online: 10February 2019

Keywords
Splicing detection, DWT, Texture, GLDM, image forgery, image authentication

***Corresponding Author**
Email:sab.mushtaq[at]gmail.com

ABSTRACT

This paper proposes a simple and fast method for splicing detection in images based on discrete wavelet transform (DWT) and statistical texture features of the image. Splicing is a common image forgery operation involving merging of two different images to create a new image to conceal or change the information conveyed by the original images. The fact that splicing forgery introduces new texture into the original image in addition to sharp transitions and abrupt changes is exploited in the proposed method. Images are firstly subjected to 3 level DWT decomposition followed by image reconstruction using the detail sub bands only. Using the original image and the reconstructed images five Gray level difference method (GLDM) texture features are obtained to form feature vectors. To lower the feature dimensionality, instead of the features their statistical mean and standard deviation is used to form the feature vector. Finally support vector machine classifier is trained to classify the test images as authentic or spliced. The proposed approach can be used to detect if a given test image is authentic or spliced with an accuracy of 92 % on CASIA image dataset and 82% on Columbia image dataset.

1. Introduction

This decade has seen a huge leap in digital imaging technology and so has the fraudulent means to create fake images. The development of photo editing software tools have made editing of images very easy that too without leaving any trace of manipulation. Among the available forgery techniques image splicing and copy-move are the two most common and easy to carry forgery techniques [1,2,3] While Splicing involves cutting and merging of two images, copy-move is copying a portion of the image and pasting it at some other place in the same image. Copy-move detection is easier than splicing detection [4] since in copy-move forgery there is a reference region in an image of which a duplicate is to be searched while in splicing detection there is no such reference region. As such developing a technique to detect splicing in images is of prime importance. An example of splicing forgery is shown in fig.1. All three images are taken from CASIA tide image dataset.

Figure1. Two images merged to form spliced image.

Number of approaches have been devised to authenticate images and are broadly classified as active methods and passive methods [1,2]. Active methods rely on digital signatures and digital watermarks which are inserted into the image during generation [5,6]. Whereas Passive authentication requires no new facts regarding the image [7,8] and is therefore achieving huge popularity. Passive methods make use of the fact that even though forgery may not be visible but it does change the underlying statistics of the image [2]. Splicing detection falls into the category of passive detection technique .The texture micro patterns of image are altered due to splicing operation [9] in addition to introduction of sharp edges and transitions. We have developed a quantifiable feature for these artifacts and employed this feature set to discriminate between authentic and spliced image. Wavelet analysis which has become an significant tool in image processing due to its superior behavior to capture sharp transitions and its multi resolution capabilities in both spatial domain and frequency domain [10] has been employed. Due to its transition capturing behavior DWT may be suitable to capture splicing in images since splicing creates transitions in image. Since the texture image also changes as a result of merging of two images, GLDM texture features are employed for texture feature extraction. GLDM texture features are relies on difference between gray levels pairs thus may be suitable to capture the texture changes that splicing introduces. The rest of the paper is organized as section 2 gives an overview on the state of art splicing detection techniques, section 3 & 4 gives brief description of DWT and GLDM techniques, Section 5 explains the proposed method and its implementation, section 6 presents and discusses the results and finally the paper is concluded in section 7.

2. Related work

Splicing disturbs the underlying statistics of the image [2], based on this a lot of research work is carried out in the direction of splicing detection based on inconsistency of features such as jpeg compression[11, 12], blur inconsistency

[13,14]15),illumination inconsistency [15], camera response function [16], noise inconsistency [17,18] . However these techniques do have certain limitation in splicing detection when post processing operations are applied. For example resizing the image before pasting it and blurring the spliced edges may remove the traces of artifacts used by above techniques. Zuo [19] method based on jpeg compression and resampling artifacts does not work well in case images are not compressed before merging. The method proposed by Kakar et al.([13] works for linear motion blur only and fails in case motion is more complex. It also fails to differentiate motion blur and out of focus blur. The method proposed by Bahrami et al.,[14] based on blur inconsistency, fails to detect multiple blur types and works for images with a single motion blur. The method proposed by Liu et al.[15] depends on the consistency of shadow illuminations however the method fails in case the lighting environment is complex as it assumes a single source of light. Splicing is known to destroy texture micro patterns in an image as reported by Hussain et al.[9]. Image texture has been reasonably used for forgery detection. Motivated by Shi et al.[19] Dong et al.[20] proposed use of edge statistics for splicing detection achieving an accuracy of 76.52% with reduced computation complexity. Hakimi et al., [21] proposed use of LBP and DWT for splicing detection reporting accuracy of 97.21 % on CASIA dataset. Shen et al. [22] proposed GLCM features of difference block DCT array to capture texture changes due to splicing. The method achieved an accuracy of 97.73% with feature dimensionality of 96. We have attempted use of Gray level difference method (GLDM) features of original image and reconstructed images which are obtained after three level DWT decomposition of original image. As reported by Tsiaparas et al., [23] the prominent texture information is held in detail sub bands. So we eliminate the approximate sub band information in the reconstructed image. Additionally the image is reconstructed from the detail wavelet sub bands only as the reconstructed image enhances the difference of authentic and spliced image [24]. A brief description of DWT and GLDM are given in next sections.

3. Discrete Wavelet Transform

Wavelet analysis is an important tool in image processing due to its superior behavior to capture sharp transitions and its multi resolution capabilities in both spatial domain and frequency domain [10]. Due to its transition capturing behavior it may be suitable to capture splicing in images since splicing creates transitions in image. DWT has been used in past for forgery detection as suggested by Chen et al., [11] using Haar transform, however this approach use all sub bands .1-level DWT of a gray-scale image is obtained as follows:

$$W(m,n) = \frac{1}{\sqrt{MN}} \sum_{x=0}^{M-1} \sum_{y=0}^{N-1} I(x,y)\Phi(x,y) \quad (1)$$

Where (M, N) is the dimensions of the image I(x, y). Φ(x, y) is defined as the scale function. W(m, n) is the approximation sub image of I(x, y) and (m, n) is the position of each pixel. Consider

$$W_i(m,n) = \frac{1}{\sqrt{MN}} \sum_{x=0}^{M-1} \sum_{y=0}^{N-1} I(x,y)\Psi_i(x,y) \quad (2)$$

A detail description of the variables is given in [23]. The input image can be divided into approximate and detail sub-bands. LL represents the approximate image and sub-bands LH, HL and HH represent the detail coefficient. To further obtain the next coarse levels the sub-band LL is decomposed. A three level DWT on of image is shown below in Fig. 2

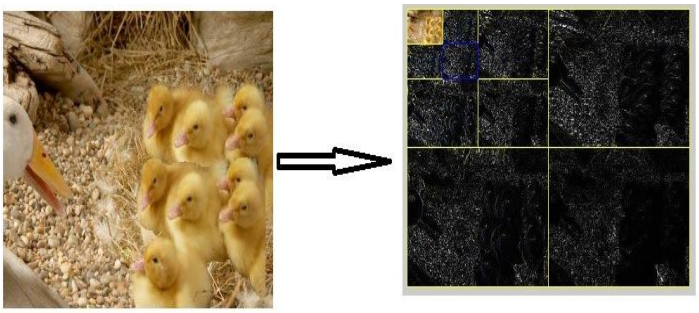

Figure 2Images and corresponding decomposition images after 3-level DWT

Considering the computation cost images are decomposed up to three levels in the proposed method. During reconstruction the original image is synthesized from the coefficients obtained in the decomposition stage. This transform is called 'Inverse Discrete Wavelet Transform' (IDWT).

4. Gray Level Difference Method (GLDM)

GLDM is concerned with the magnitude of difference of co-occurring gray level pixels. GLDM may be described (Mir et al.,1995; Weszka et al.,1976) on a digital image f(x,y) for a displacement 'δ' = (Δx,Δy), where Δx and Δy are integers, as fΔ(x,y)= |f(x,y)-f(x+Δx,y+Δy)|. Let ĝ (i/δ) be the estimated probability density function associated with values of i of 'f', i.e.

$$\hat{g}(i/\delta) = P(f_\delta(x,y)=i) \quad (3)$$

It is easy to compute ĝ (i/δ)from image f(x,y) by calculating the number of times each value of fΔ(x, **y)** occurs, where Δx and Δyare integers. This method considers four possible forms of δ They are (0,d),(-d,d),(d,0) and (-d,-d) where d is the inter sample spacing distance and we have used d=1in the proposed method. We will refer to the functions ĝ (i/δ) as the gray level difference density functions. From each of these density functions five texture features are defined. They are as follows.

$$\text{Contrast} = \sum_{i=0}^{Ng-1} i^2 \hat{g}(i/\delta) \quad (4)$$

$$\text{Angular Second Moment} = \sum_{i=0}^{Ng-1} [\hat{g}(i/\delta)]^2 \quad (5)$$

$$\text{Entropy} = \sum_{i=0}^{Ng-1} \hat{g}(i/\delta) \log\left(\hat{g}\left(\frac{i}{\delta}\right)\right) \quad (6)$$

$$\text{Mean} = \sum_{i=0}^{Ng-1} i\, \hat{g}(i/\delta) \quad (7)$$

$$\text{Inverse Difference Moment} = \sum_{i=0}^{Ng-1} \frac{\hat{g}(i/\delta)}{(i^2+1)} \quad (8)$$

GLDM is based on difference between gray level pairs thus may be suitable to capture the texture changes that splicing introduces.

5. Proposed Approach & Implementation

The proposed method makes use of wavelet analysis. Wavelet analysis captures inconsistencies caused by splicing

since splicing creates sharp transitions and boundaries. We have attempted possible detection of splicing using wavelet analysis and texture features as it has not been attempted before. The method extracts GLDM texture features from image to classify it as authentic or spliced. The suggested technique is diagrammatically shown in Fig. 3. Implementation is discussed in below sub-sections.

5.1 Database: The publically available dataset for splicing are CASIA [26] and Columbia Dataset provided by DVMM, Columbia University [27]. The details of both are given in table 1 below.

Table 1
Training and Testing data

Database	Natural images	Spliced images	Training Set		Testing Set	
			Natural	Spliced	Natural	Spliced
CASIA	800	921	668	767	133	153
Columbia	933	912	776	760	155	154

The datasets are designed so as to benchmark the blind splicing detection algorithms. All experiments in this paper are conducted on these two datasets.

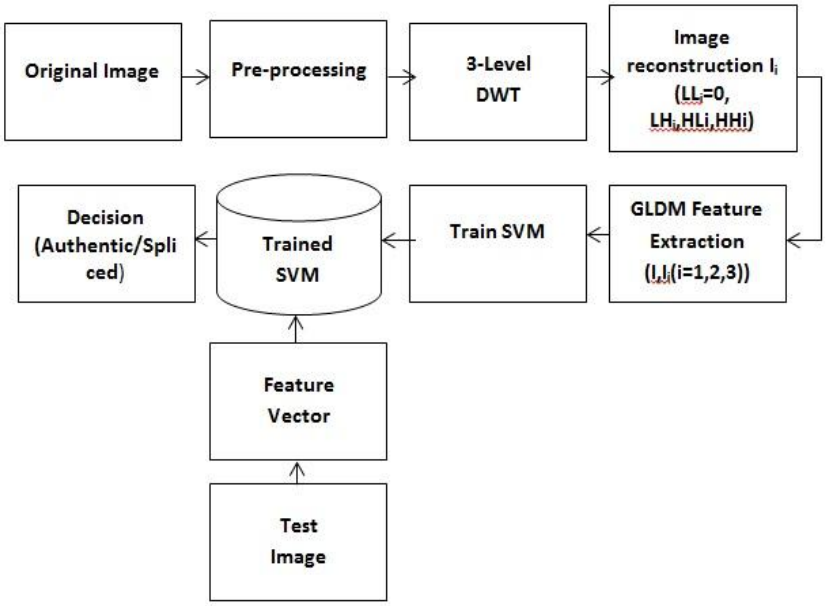

Figure3: Proposed method for splicing detection

5.2 Pre-Processing

The input RGB image is first converted to YCbCr color space. It characterizes an image into luminance component(Y) and chrominance component (Cb or Cr). Image content is mostly preserved in Y component and hides the tampering traces strongly [28]. The splicing caused edges are more detectable in chroma component Wang[28]. The edges caused by splicing are emphasized in chroma channel Kaur & Gupta[29]. Furthermore Chrominance components are a good texture representations than the gray level or luminance component in YCbCr [30].

Hence further processing is performed on all three channel of YCbCr. The conversion is done using formula:

$$\begin{pmatrix} Y \\ Cb \\ Cr \end{pmatrix} = \begin{pmatrix} .299 \\ -.299 \\ .701 \end{pmatrix} \begin{pmatrix} .587 \\ -.587 \\ -.587 \end{pmatrix} \begin{pmatrix} .117 \\ .886 \\ .114 \end{pmatrix} + \begin{pmatrix} 16 \\ 128 \\ 128 \end{pmatrix} \quad (9)$$

Y is the weight sum of *R, G*, and *B* channels; Cb is the blue difference and Cr channels red-difference components. Splicing detection in images is regarded as detection of weak signals in presence of strong image content. Thus detection of splicing is not preferred in Y channel since it reserves maximum image content. On the contrary, Chroma channel holds less image content and it therefore suitable for detection of splicing traces.

5.3 DWT Decomposition and Image Reconstruction

3-level DWT using Daubechies wavelet is applied to Y , Cb and Cr image component and to the gray scale images from CASIA dataset yielding approximate high scale low frequency component (LL) and detail low scale high frequency components at each level(LH,HL,HH). After DWT decomposition images RI_i (i=1,2,3) are reconstructed by removing the content in sub-band LL_i (i=1,2,3). The reason for using reconstructed image is to enhance the difference between authentic image and spliced image [23] and to weaken the residual image content. The reconstructed image is an edge image that contains the edge information of the original image.

5.4 GLDM Feature Extraction

The textural feature based on statistics encapsulates the relative distribution of frequency. Five textural features (ASM, Mean, Entropy,Contrast and IDM) are extracted from GLDM for a chosen distance d =1 in four directions (θ= 0°, 45°, 90°,135°). Textural features are calculated from the original image and the corresponding reconstructed images after DWT decomposition. These features are calculated at {d=1,θ= 0°},{d=1,θ= 45°},{d=1,θ= 90°},{d=1,θ= 135°}. Traditionally the features extracted from GLDM are directly used as features. However in order to better describe the relationship between pixels and the distribution properties of intensity in nature mean and standard deviation are calculated over the similar feature types. Hence a set of {Me_1, SD_1,Me_2,SD_2,Me_3,SD_3,Me_4,SD_4,Me_5,SD_5, } from all five features based on GLDM in four directions is obtained forming a 10 dimension feature vector as shown in Fig 4. Similarly 10-D feature vector for each RIi (i=1, 2, 3) is calculated. Finally, we concatenate the four 10-D feature vectors obtained for the original image and reconstructed images to get a 40-D feature vector for splicing detection in images as shown in Fig 5.

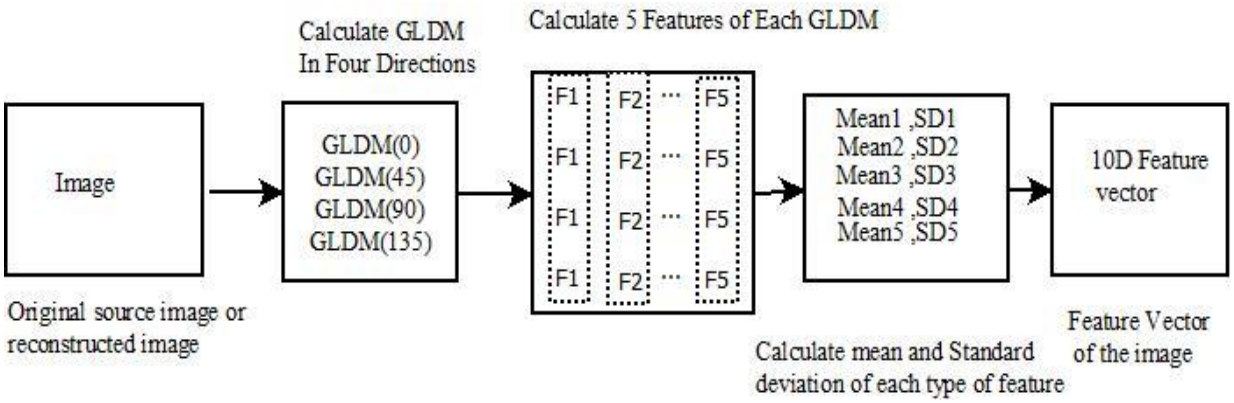

Figure 4:Feature Extraction Step

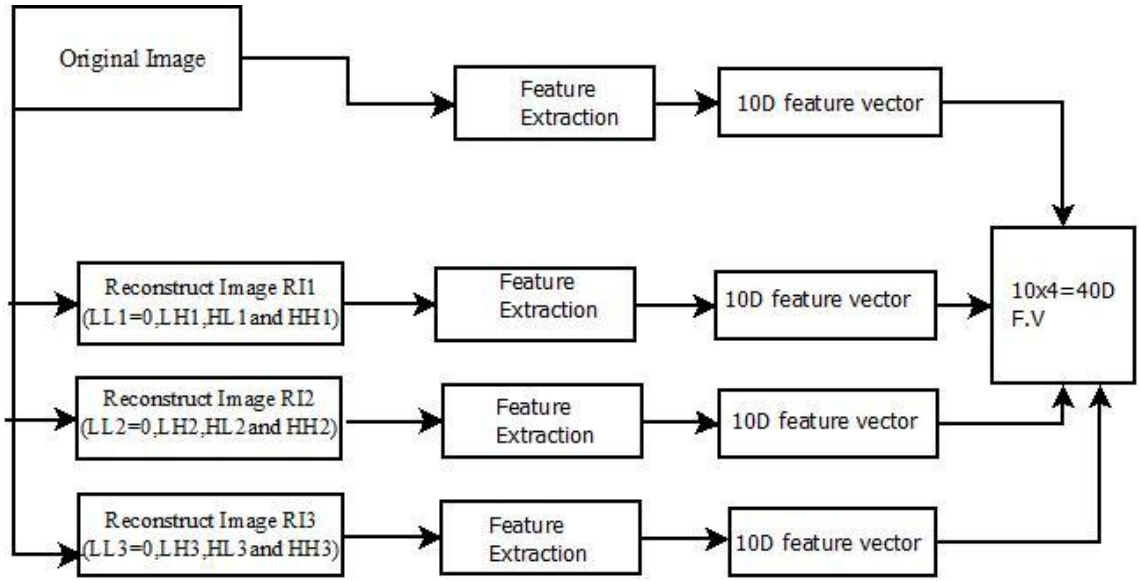

Figure 5: 40- D Feature vector generation procedure in the proposed method.

5.5 Classifier

Support vector machine is utilized as the classifier in our experiments, using RBF kernel. We have used LS-SVM [31]. In the experiments, all the authentic images are labeled as +1 (positive), while all the spliced images are labeled as -1 (negative). Then the classification of images into authentic and spliced images becomes a binary decision problem.

Software platform used for experimentation is MatlabR2009b on windows7 core i3 processor PC. We have conducted 20 independent tests. In each test set 5/6 authentic images and 5/6 spliced images are used to train SVM and the remaining 1/6 of the images are used for testing the classifier. The average of the 20 tests forms the final result. Performance measures calculated to evaluate the method are True positive rate (TPR), True negative rate (TNR), accuracy and receiver operating characteristics (ROC) curve.

5.6 Performance Evaluation

In binary classification the results are labeled either as P Or N . There are four possible outcomes. True Positive(TP),True Negative(TN), False Positive(FP) and False Negative(FN) where TP and TN means the predicted value is actual value and if the actual value is N and predicted value is P then it is said to be a false positive (FP) and False Negative (FN) is when the predicted outcome is N and actual value is P.

Performance measures calculated to evaluate the method are True positive rate (TPR), True negative rate (TNR), accuracy and receiver operating characteristics (ROC) curve.

True Positive Rate:

$$TPR = \frac{TP}{TP+FN} \times 100$$

True Negative Rate

$$TNR = \frac{TN}{TN+FP} \times 100$$

Accuracy: It is average value of TPR and TNR

$$Accuracy = \frac{TP+TN}{TP+TN+FP+FN} \times 100$$

6. Results & Comparison

Experimental results are presented in order to validate the proposed method. The proposed method is evaluated on CASIA. TPR, TNR and accuracy are used to evaluate the results. Different combinations of Y, Cb and Cr are considered. In each channel experiment the 40-D feature vector is calculated according to the above described approach.

Table 2 shows the results of different channels for splicing detection as performed on CASIA dataset

Table 2
Detection Results obtained on CASIA dataset

Channel	TPR	FPR	Precision	AUC	F1-Score	Accuracy	Feature Dimension
Y	78.00	12%	88.14%	.872	82.6%	83%	40
Cb	90.1	7%	93.24%	.932	91.6%	91.5%	40
Cr	91.00	6.5%	93.9%	.958	92.3%	92 %	40

The results obtained using Columbia dataset is shown below in table 3. Images available in Columbia dataset are gray scale images as such the suggested method is evaluated for gray scale images as well.

Table 3
Detection Results obtained on Columbia dataset

Channel	TPR	FPR	Precision	AUC	F1-Score	Accuracy
Gray	83.00%	18.5%	81.5	.85	82.3%	82.2 %

From table 2 and 3 it can be noted that in terms of accuracy in single channel, accuracy using gray images gives poor detection accuracy. The highest detection accuracy is achieved by feature extraction in Cr channel. Corresponding ROC curve is shown in figure 6. ROC curves typically features true positive rate on the Y axis, and false positive rate on the X axis. ROC curve is a graphical illustration for the performance of a binary system. In machine learning TPR is also known as Sensitivity and FPR is also known as Specificity.

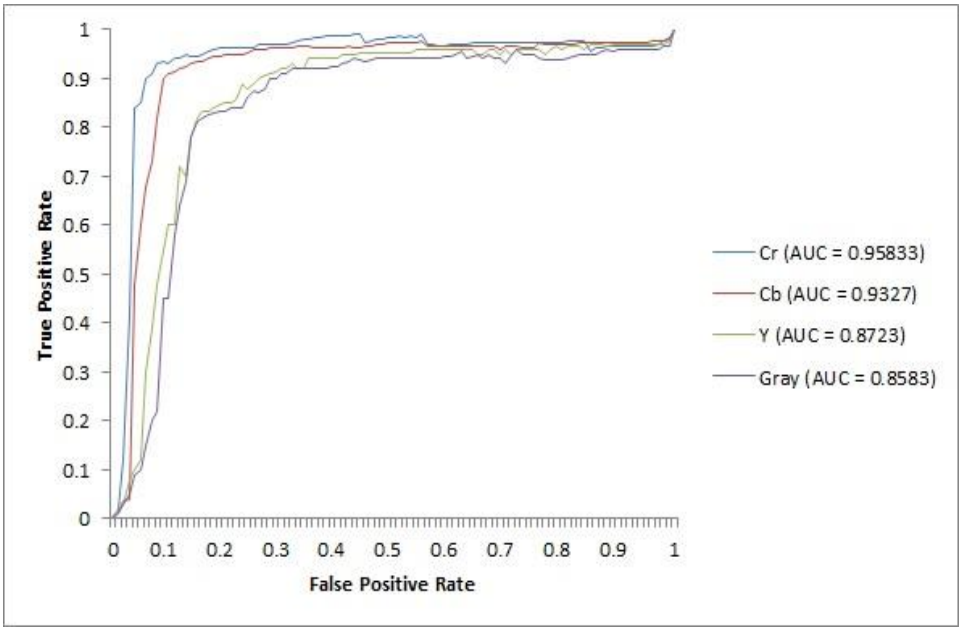

Figure 6:ROC curve

From table 2 and table 3 and Fig 3.11 we can see that the detection accuracy of proposed method is higher for CASIA dataset than for Columbia dataset. One reason may be due to the small size of images (128x128) in Columbia dataset as compared to CASIA image (384x256) and second reason is that images in CASIA dataset are evaluated in YCbCr

channels while in Columbia images being gray scale are evaluated as such. The ROC curve shows an accuracy of 92% for Cr channel in CASIA dataset. However performance for Columbia dataset is 82 % only.

Comparison

For comprehensive evaluation of the proposed technique, we compare the results obtained using the proposed method with some state of art image splicing detection techniques. The comparison of the proposed approach to the recent methods is tabulated below in table 4. The features extracted by the methods are also shown. The comparison results are as reported by the original papers. As shown by the table the proposed method performs reasonably well in comparison to other methods. Though the detection accuracy for methods proposed by Muhammad et al.(2014)]and Shen et al.(2016) are better. However the feature dimension of both methods Muhammad et al.(2014) and Shen et al.(2016) is nearly double that of our proposed method. When compared to other methods, our method performs better in terms of detection accuracy as well as feature dimension.

Table 4:
Comparison results of the proposed technique and other methods.

Method	Feature used	Feature Dimension	Accuracy	
			CASIA	Columbia
Dong et al.[20]	Run length and edge statistics	61		76.52%
He et al.[24]	Approx. run length	30	-	80.58%
He et al.[2]	Markov Features	100	89.76%	-
Shen et al.[22]	TF-GLCM	96	97.73%	-
Kaur & Savita[29]	DWT+LBP	1024	92.62%	75.93%
Muhammad et al.[32]	Gabor + DCT	70	97.90%	-
Proposed Method	GLDM	40	92%	82%

7. Conclusion

In this paper a splicing detection method based on DWT and texture features is proposed. DWT is able to capture sharp transitions in image while GLDM capture texture changes introduced in the image as a result of splicing process. Firstly the image is subjected to three level DWT followed by image reconstruction from the detail sub bands zeroing the approximate details. Texture feature GLDM is calculated for the image and the reconstructed images in four directions. Mean and standard deviation of which are fed to train SVM classifier to classify a test image as authentic or spliced. The proposed technique is evaluated using two standard datasets CASIA and Columbia yielding highest detection accuracy of 92% in chrominance channel and 82% for gray images. Compared to other methods suggested method performs reasonably well in terms of both detection accuracy and feature dimension as well. We thus believe that this approach can be thus used in the digital image forensics field.

References

1. Al-Qershi, Osamah M., and Bee Ee Khoo. "Passive detection of copy-move forgery in digital images: State-of-the-art." *Forensic science international*231.1 (2013): 284-295.
2. He, Zhongwei, Wei Lu, Wei Sun, and Jiwu Huang. "Digital image splicing detection based on Markov features in DCT and DWT domain." *Pattern Recognition* 45, no. 12 (2012): 4292-4299.
3. Mushtaq, Saba, and Ajaz Hussain Mir. "Digital image forgeries and passive image authentication techniques: A survey." *International Journal of Advanced Science and Technology* 73 (2014): 15-32.
4. Hu, Wu-Chih, Jing-Siou Dai, and Jhih-Syuan Jian. "Effective composite image detection method based on feature inconsistency of image components." *Digital Signal Processing* 39 (2015): 50-62.
5. Rey, Christian, and Jean-Luc Dugelay. "A survey of watermarking algorithms for image authentication." *EURASIP Journal on Advances in Signal Processing* 2002, no. 6 (2002): 218932.
6. Fridrich. J, Methods for tamper detection in digital images, in: Proceedings of the ACM Workshop on Multimedia and Security, (1999), pp. 19–23.
7. Fridrich, A. Jessica, B. David Soukal, and A. Jan Lukáš. "Detection of copy-move forgery in digital images." In *in Proceedings of Digital Forensic Research Workshop*. 2003.
8. Luo, Weiqi, Zhenhua Qu, Feng Pan, and Jiwu Huang. "A survey of passive technology for digital image forensics." *Frontiers of Computer Science in China* 1, no. 2 (2007): 166-179.
9. Hussain, Muhammad, Sahar Q. Saleh, Hatim Aboalsamh, Ghulam Muhammad, and George Bebis. "Comparison between WLD and LBP descriptors for non-intrusive image forgery detection." In *Innovations in Intelligent Systems and Applications (INISTA) Proceedings, 2014 IEEE International Symposium on*, pp. 197-204. IEEE, 2014.
10. Xu, Yansun, John B. Weaver, Dennis M. Healy, and Jian Lu. "Wavelet transform domain filters: a spatially selective noise filtration technique." *IEEE transactions on image processing* 3, no. 6 (1994): 747-758.
11. Zuo, Juxian, Shengjun Pan, Benyong Liu, and Xiang Liao. "Tampering detection for composite images based on re-sampling and JPEG compression." In *Pattern Recognition (ACPR), 2011 First Asian Conference on*, pp. 169-173. IEEE, 2011.

12. Bianchi, Tiziano, and Alessandro Piva. "Image forgery localization via block-grained analysis of JPEG artifacts." *IEEE Transactions on Information Forensics and Security* 7, no. 3 (2012): 1003-1017.
13. Kakar, Pravin, Natarajan Sudha, and Wee Ser. "Exposing digital image forgeries by detecting discrepancies in motion blur." *IEEE Transactions on Multimedia* 13, no. 3 (2011): 443-452.
14. Bahrami, Khosro, Alex C. Kot, Leida Li, and Haoliang Li. "Blurred image splicing localization by exposing blur type inconsistency." *IEEE Transactions on Information Forensics and Security* 10, no. 5 (2015): 999-1009.
15. Liu, Qiguang, Xiaochun Cao, Chao Deng, and Xiaojie Guo. "Identifying image composites through shadow matte consistency." *IEEE Transactions on Information Forensics and Security* 6, no. 3 (2011): 1111-1122.
16. Hsu, Y.F. and Chang, S.F., 2010. Camera response functions for image forensics: an automatic algorithm for splicing detection. *IEEE Transactions on Information Forensics and Security*, *5*(4), pp.816-825.
17. Mahdian, Babak, and Stanislav Saic. "Using noise inconsistencies for blind image forensics." *Image and Vision Computing* 27, no. 10 (2009): 1497-1503.
18. A.C. Popescu, Statistical tools for digital image forensics, Ph.D. Dissertation, Department of Computer Science, Dartmouth College, Hanover, NH, 2005.
19. Shi, Yun Q., Chunhua Chen, and Wen Chen. "A natural image model approach to splicing detection." *Proceedings of the 9th workshop on Multimedia & security*. ACM, 2007.
20. Dong, Jing, Wei Wang, Tieniu Tan, and Yun Q. Shi. "Run-Length and Edge Statistics Based Approach for Image Splicing Detection." In *IWDW*, pp. 76-87. 2008.
21. Hakimi, Fahime, Mahdi Hariri, and Farhad GharehBaghi. "Image splicing forgery detection using local binary pattern and discrete wavelet transform." In *Knowledge-Based Engineering and Innovation (KBEI), 2015 2nd International Conference on*, pp. 1074-1077. IEEE, 2015.
22. Shen, Xuanjing, Zenan Shi, and Haipeng Chen. "Splicing image forgery detection using textural features based on the grey level co-occurrence matrices." *IET Image Processing* 11, no. 1 (2016): 44-53.
23. Tsiaparas, Nikolaos N., Spyretta Golemati, Ioannis Andreadis, John S. Stoitsis, Ioannis Valavanis, and Konstantina S. Nikita. "Comparison of multiresolution features for texture classification of carotid atherosclerosis from B-mode ultrasound." *IEEE Transactions on Information Technology in Biomedicine* 15, no. 1 (2011): 130-137.
24. He, Zhongwei, Wei Sun, Wei Lu, and Hongtao Lu. "Digital image splicing detection based on approximate run length." *Pattern Recognition Letters* 32, no. 12 (2011): 1591-1597.
25. Chen, Wen, Yun Q. Shi, and Wei Su. "Image splicing detection using 2-D phase congruency and statistical moments of characteristic function." In *Security, Steganography, and Watermarking of Multimedia Contents*, p. 65050R. 2007.
26. Dong, Jing, and Wei Wang. "CASIA tampered image detection evaluation database." (2011).
27. Ng, T.-T., Chang, S.-F., 2004. A data set of authentic and spliced image blocks. Tech. Rep. 203-2004-3, Columbia University.
28. Wang, W., Dong, J. and Tan, T., 2009, November. Effective image splicing detection based on image chroma. In *Image Processing (ICIP), 2009 16th IEEE International Conference on* (pp. 1257-1260). IEEE.
29. Kaur, Mandeep, and Savita Gupta. "A Passive Blind Approach for Image Splicing Detection Based on DWT and LBP Histograms." *International Symposium on Security in Computing and Communication*. Springer Singapore, 2016. In: Mueller P., Thampi S., Alam Bhuiyan M., Ko R., Doss R., Alcaraz Calero J. (eds)
30. Alahmadi, Amani A., Muhammad Hussain, Hatim Aboalsamh, Ghulam Muhammad, and George Bebis. "Splicing image forgery detection based on DCT and Local Binary Pattern." In *Global Conference on Signal and Information Processing (GlobalSIP), 2013 IEEE*, pp. 253-256. IEEE, 2013.
31. De Brabanter, K., Karsmakers, P., Ojeda, F., Alzate, C., De Brabanter, J., Pelckmans, K., De Moor, B., Vandewalle, J. and Suykens, J.A., 2010. *LS-SVMlab Toolbox User's Guide: version 1.7*. Katholieke Universiteit Leuven.
32. Muhammad, Ghulam, M. Solaiman Dewan, M. Moniruzzaman, Muhammad Hussain, and M. Nurul Huda. "Image forgery detection using Gabor filters and DCT." In *Electrical Engineering and Information & Communication Technology (ICEEICT), 2014 International Conference on*, pp. 1-5. IEEE, 2014.

